REPORT DOCUMENTATION PAGE

Form Approved OMB No. 0704-0188

1. REPORT DATE *(DD-MM-YYYY)*	2. REPORT TYPE	3. DATES COVERED *(From – To)*
07-10-2008	Final Report	15 August 2007 - 28-Jan-10

4. TITLE AND SUBTITLE

Ultra High Temperature Ceramics for Aerospace Use

5a. CONTRACT NUMBER
FA8655-07-1-3087

5b. GRANT NUMBER

5c. PROGRAM ELEMENT NUMBER

6. AUTHOR(S)

Professor Julian Martínez Fernández

5d. PROJECT NUMBER

5d. TASK NUMBER

5e. WORK UNIT NUMBER

7. PERFORMING ORGANIZATION NAME(S) AND ADDRESS(ES)

University of Seville
Av/ Reina Mercedes s/n, Apdo. 1065
Sevilla 41080
Spain

8. PERFORMING ORGANIZATION REPORT NUMBER

N/A

9. SPONSORING/MONITORING AGENCY NAME(S) AND ADDRESS(ES)

EOARD
Unit 4515 BOX 14
APO AE 09421

10. SPONSOR/MONITOR'S ACRONYM(S)

11. SPONSOR/MONITOR'S REPORT NUMBER(S)
Grant 07-3087

12. DISTRIBUTION/AVAILABILITY STATEMENT

Approved for public release; distribution is unlimited.

13. SUPPLEMENTARY NOTES

14. ABSTRACT

This report results from a contract tasking University of Seville as follows: The poor oxidation resistance of UHTCs is the predominant factor limiting their applicability to aerospace applications. The purpose of this study is to perform an extensive research of these materials under conditions representative of propulsion environments, that will lead to an understanding of process that will improve these materials performance. The initial materials to be studied will be ZrB2 plus 20 vol.% SiC (abbreviated as ZS), ZrB2 plus 14 vol.% SiC plus 30 vol.% C (ZSC), and SCS-9a SiC fiber reinforced ZrB2 plus 20 vol.% SiC (ZSS). The PI proposes a program with four broad, integrated objectives to be pursued each one with the others feed-back. These objectives are:
1.Determination of the mechanical behavior of these Ultra High Temperature Ceramics by compression tests. It must be noted that there is no data under these solicitation conditions in the literature. The knowledge of the dependence of mechanical properties with stress, temperature and time at temperature will be expressed as a phenomenological equation, that will allow the mechanical behavior prediction in other conditions.
2.Study in depth of the as-fabricated materials microstructure, and its evolution after mechanical tests, using a wide variety of characterization techniques. Determination of the optimal microstructure to minimize residual stresses.
3.Understanding of the correlation beteween microstructure, properties and thermal history.
4.Modifications on the fabrication process will be suggested, at the end of this one year period, to further improve the UHTC properties.

15. SUBJECT TERMS
EOARD, ultra high temperature ceramics

16. SECURITY CLASSIFICATION OF:			17. LIMITATION OF ABSTRACT	18, NUMBER OF PAGES	19a. NAME OF RESPONSIBLE PERSON
a. REPORT	b. ABSTRACT	c. THIS PAGE			WYNN SANDERS, Maj, USAF
UNCLAS	UNCLAS	UNCLAS	UL	21	19b. TELEPHONE NUMBER *(Include area code)* +44 (0)1895 616 007

ULTRA HIGH TEMPERATURE CERAMICS FOR AEROPROPULSION AND AEROSPACE USE
Final report of grant #FA8655-07 -1-3087

PI: Julián Martínez Fernández
Departamento de Física de la Materia Condensada
University of Seville, Sevilla, SPAIN

This material is based upon work supported by the European Office of Aerospace Research and Development, Air Force Office of Scientific Research, Air Force Research Laboratory, under Grant No. FA8655-07 -1-3087. Any opinions, findings and conclusions or recommendations expressed in this material are those of the author(s) and do not necessarily reflect the views of the European Office of Aerospace Research and Development, Air Force Office of Scientific Research, Air Force Research Laboratory.

Table of Contents

Summary

The high melting point of refractory metal diborides makes them promising materials for ultra high temperature applications. In this work, we study the mechanical strength of ZrB_2-SiC composites with variable amounts of additive Carbon, the SiC phase being in grain and fiber morphologies. Samples have been studied in compression at room temperature, 1400ºC and 1550ºC, in atmospheric air. The degradation of the mechanical properties as a result of atmospheric air exposure at high temperatures has also been studied as a function of exposure time. In the fiber composite the matrix presents significant microcracking due to residual thermal stresses, and therefore shows poor mechanical properties. Strength in the polycrystalline compositions is highly influenced by the presence of carbon, as it burns out at high temperatures. After exposure to air at high temperatures a SiO_2 layer is formed, below which ZrB_2 oxidizes to ZrO_2. A reduction of 30% in room temperature strength occurs after 16-24h of exposure to air at 1400ºC for the ZrB_2-SiC material, while for the ZrB_2-SiC-C composition it occurs after less than 6h. The thickness of the oxide layer has been measured and the oxidation process is discussed in terms of the existing models.

Introduction

The high melting point of refractory metal diborides coupled with their ability to form refractory oxide scales give these materials the capacity to withstand temperatures in the 1900-2500ºC range. These Ultra-High Temperature Ceramics (UHTC) were developed in the 1960s [1]. Fenter [2] provides a comprehensive review of the work accomplished in the 1960s and early 1970s. Additions of Silicon Carbide are used to enhance oxidation resistance and limit diboride grain growth. Carbon is also sometimes used as an additive to enhance thermal stress resistance.

These materials offer a good combination of properties that make them candidates for airframe leading edges on sharp bodied reentry vehicles [3]. UHTCs have some potential to perform well in such applications' environment, i.e. air at low pressure. However, for hypersonic flight in the upper atmosphere one must recognize that stagnation pressures can be greater than one atmosphere. Some interest has also been shown in these materials for single use propulsion applications [4]. Preliminary studies [5] of oxidation resistance and mechanical properties by bending tests indicate that processing does not seem to be under full control, as evidenced by the large scatter in mechanical property data. The key to raising their potential for any application is to improve the processing route and thus material reproducibility, through an understanding of the correlation between processing, microstructure and mechanical properties, area in which major improvements are needed.

In this work, we study the mechanical strength of ZrB_2-SiC composites with variable amounts of additive Carbon, the SiC phase being in grain and fiber morphologies. Samples have been studied in compression at room temperature, 1400ºC and 1550ºC, in atmospheric air. The degradation of the mechanical properties as a result of atmospheric air exposure at high temperatures has also been studied as a function of exposure time. The microstructure and composition of the as-fabricated and tested materials has been studied by means of Scanning Electron Microscopy (SEM) and Energy Dispersive Spectroscopy (EDS).

Methods, Assumptions, and Procedures

Samples of ZrB_2-SiC composites were fabricated using a technique previously described elsewhere [5, 6]. Two polycrystalline composites were studied, containing variable amounts of ZrB_2 and SiC; one of them also contained C. A third, fiber-reinforced composite consisting of SCS-9a SiC fibers in a ZrB_2-C matrix was also studied. The nominal compositions of the materials investigated are summarized in Table 1.

Compression tests were carried out on an electromechanical universal testing machine with a furnace attached in its frame. Load was applied using alumina rods with SiC pads. Samples were cut into parallelepiped shape using a low speed diamond saw. Nominal sample dimensions were 3x3x5 mm, and the load was applied to the longest dimension. High temperature mechanical tests were conducted at room temperature, 1400ºC and 1550ºC. Several samples were exposed to oxidation by annealing at 1400ºC in atmospheric air, and exposure times ranged from 6h to 48h. The room temperature strength was measured after annealing, to study the degradation of the mechanical properties after exposure to an oxidizing environment

Microstructural studies were carried out using SEM and EDS techniques, in both the as-fabricated and tested specimens. Samples were prepared using conventional metallographic techniques which involved cutting, grinding and lapping. A conductive coating of either carbon or gold was applied to the specimens prior to observation.

Results and discussion

Microstructure of as-received specimens

Figure 1 shows the as fabricated microstructure of all studied compositions. Our observations match those reported in [5]. The ZS composite appears to be fully dense (figure 1.A), while the ZSC suffered from significant grain pullout during polishing, as evidenced in figure 1.B. This is attributed to the weak C bonding to the ZrB_2 and SiC, phases, which results in removal of the

C phase during grinding. The fiber composite microstructure is shown in figures 1.C and 1.D. Fibers were disposed in layers of approximately hexagonal packing, although some layers were more ordered than others. It can be seen that the fiber coating remained intact during the uniaxial pressing step of the fabrication route. The ZrB_2-C matrix was highly porous, although is difficult to ascertain whether this is due to grain pullout, as in the ZSC composite, or due to the fabrication route. Previous studies estimated this porosity to be present on the as-fabricated material, and amounted for 40% volume of the matrix.

From figure 1.C it can be seen that the matrix showed significant cracking in the ZSS material, with penny shaped circular cracks perpendicular to the fiber direction. A detailed view is presented in figure 2. This is a consequence of the thermal expansion mismatch between the fibers and the matrix, which creates residual stresses during material cool-down from the sintering temperature. The relevant physical properties of the constituent phases are presented in Table 2. The matrix is highly porous and therefore must have a low strength, which in turn causes the thermal stresses to relax through microcracking. This effect was not observed in the ZSC composite, because its polycrystalline character makes the stress distribution isotropic.

The amount of cracks in the ZSS composite could be lowered by engineering the spatial distribution of fibers in the composite in such a way that makes the stress distribution less anisotropic. FEM simulations aimed to design the most appropriate fiber geometry are currently in progress.

Figure 3 shows elemental maps of the ZSS composite obtained by EDS. It can be seen that the SCS-9a fibers contain a carbon core surrounded by SiC. The whole fiber is carbon coated, as it is seen in the elemental C Kα map. No impurities were observed in the as-fabricated material, up to the detection limit of the technique (0.1 wt. %).

High Temperature Strength

The high temperature compressive strength was measured at 1400ºC and 1550ºC in atmospheric air for all the studied compositions. Figure 4 and 5 summarize the measured strength for 1400ºC and 1550ºC temperatures, respectively. Due to matrix porosity and microcracking, the ZSS composite exhibited the lowest strength of all three. The ZS composite is seen to be more resistant than the carbon containing ZSC. This is attributed to both the weak carbon bonding to the other phases, evidenced as grain pullout in the SEM observations, and the burnout of carbon at high temperature in air. This creates porosity and also produces channels through which air can enter, oxidizing the ZrB_2 phase not only on the surface but also inside the sample. At 1550ºC, creep of the SiC pads used as a protection to the alumina rods could be observed at high stresses. For the ZSC material this effect was of little importance because the strengths were quite low, but was significant in the ZS material. For this

reasons, we quote our result as a minimum strength. In some cases the SiC pads broke, leaving the sample intact.

Failure mode at high temperatures is depicted in figure 6. In general, the fracture surface in ZS samples was diagonal (figure 6.A), at an angle with respect to the applied stress, while in ZSC fracture surface was usually parallel to the load direction (figure 6.B). The failure mode of ZSS could be described as debonding and buckling of the fiber layers (see below)

After deformation at high temperature, the samples appeared to be coated by a glassy phase, which was confirmed to be SiO_2 by EDS analysis. Figure 7 shows the surface of a ZSS composite deformed at 1550ºC. Figure 7.A is a general view, in which the glassy phase can be seen to cover the sample. Figure 7.B is a detailed view of the fibers. It can be seen that the carbon core of the fiber is sometimes burned, and that some of the fibers have oxidized completely. Figure 8 shows a cross section of a ZS specimen deformed at 1550ºC (BSE contrast); two different layers can be seen, the top one consisting of SiO_2 and some ZrO_2 and the bottom one consisting of mostly ZrO_2.The layers' composition was confirmed by EDS. Both layers were covered by an outer SiO_2 layer.

At 1400ºC, the samples were also covered by SiO_2 but not completely as in the previous case. This allowed us to observe the microstructure of some exposed surfaces, as can be seen in figure 9, for a ZS composite. ZrO_2 grains can be seen in place of the ZrB_2 grains, as well as SiC grains (compare this with figure 1.A). In general, our observations are consistent with those of [5].

Room Temperature Strength and Degradation

The degradation in the mechanical properties was studied as a function of exposure time to atmospheric air at 1400ºC. Since the ZSS composite showed such a poor mechanical performance, we decided to focus on the two other compositions. Figures 10 and 11 show some selected stress-strain curves for ZS and ZSC, respectively, for exposure times ranging from 0 to 48h at 1400ºC in atmospheric air. These results are summarized in figure 12, where the room temperature strength of the materials is plotted as a function of exposure time. For ZS, a reduction of 30% in strength occurred between 16h and 24h, while for ZSC less than 6 hours were needed. This can be explained considering that C burns in an oxidizing atmosphere, creating pores and channels through which air can permeate. At present we can not explain the increase in strength for ZS after 6h exposure; further tests will be carried out to ascertain whether this is an intrinsic effect or rather an effect of the low reproducibility of these materials [5].

Figure 13 shows the fracture surface of ZS and ZSC after 6h exposure. In general failure was intergranular. No significant differences could be observed

in SEM. Work is progress to perform TEM studies to observe the grain boundaries, as it is likely that oxidation occurred.

Oxide layer formation

The microstructure and thickness of the oxide layers formed after exposure to atmospheric air at 1400ºC was studied for both ZS and ZSC samples, which were cut and polished for observation in the SEM. Figure 14 shows a micrograph and compositional maps for a ZS sample annealed for 1 hour. The outer, Si and O rich layer can be concluded to be SiO_2, while the intermediate layer, which is O rich and B poor, is ZrO_2. Similar conclusions can be drawn from Figure 15, which represents compositional maps for a ZSC sample annealed for 24h. Again, the outer layer is mainly composed of SiO_2, and an intermediate layer of ZrO_2 separates the former layer and the bulk interior of the sample.

These observations were confirmed by quantitative analysis, of which an example is presented. Figure 16 is a cross section of a ZSC sample annealed for 24h at 1400ºC in air, and contains several of the features previously observed. The microstructure of the oxide layer can be divided into four different zones or regions. The first and outer one is composed of ZrO_2 grains embedded in a glassy SiO_2 matrix, as can be deduced from the elemental composition, depicted in Figure 17. This matches our previous observations, such as that of Figure 8. The Zone labeled as number 2 is composed only of SiO_2, while the zone labeled as 3 is composed almost exclusively of ZrO_2 and contains no Si. The fourth zone corresponds to the composition of the bulk, as fabricated material. For ease of comparison, raw spectra obtained from all four different zones are depicted in Figure 18.

These observations confirm the oxidation process already outlined in previous references, such as [5]. Both ZrB_2 and SiC are oxidized, producing B_2O_3 that evaporates at high temperatures. The SiO_2 formed, which is liquid at the studied temperatures, is expelled towards the surface of the sample by capillary forces, and acts as a protective layer. The intermediate layer is thus composed mostly of ZrO_2 and pores that allow for oxygen permeation. It is thus expected that the ZSC samples, containing carbon that burns out at high temperature, will oxidize at a faster rate because of the porosity produced during carbon combustion.

To ascertain this effect, the thickness of both the SiO_2 and ZrO_2 oxide layers were measured as a function of annealing time, for both ZS and ZSC samples. These results are presented in Figures 19 and 20, respectively. It can be seen that the reaction rate is faster for samples containing C, and that the thickness of the oxide layers is smaller for ZS samples.

Conclusions

The mechanical properties of the ZrB_2-SiC materials studied are highly dependent on both the geometry of the constituent phases and the amount of C, when exposed to oxidizing environments at high temperatures. The ZS composition shows the best performance on the three compositions studied, both in terms of strength and oxidation resistance. The ZSS composite performs very poorly due to the cracks induced by the thermal residuals stresses. Selecting a different fiber arrangement during manufacturing or making the ZrB_2-C matrix denser could alleviate this problem. The ZS material can withstand exposures up to 24h in air at 1400ºC before its performance is significantly degraded, but the ZSC composition is probably not suitable for application if no protective coating is applied.

Acknowledgments

This material is based upon work supported by the European Office of Aerospace Research and Development, Air Force Office of Scientific Research, Air Force Research Laboratory, under Grants No. **FA8655-07 -1-3087**. Any opinions, findings and conclusions or recommendations expressed in this material are those of the author(s) and do not necessarily reflect the views of the European Office of Aerospace Research and Development, Air Force Office of Scientific Research, Air Force Research Laboratory. The authors want to acknowledge the collaboration of NASA-Glenn, CITIUS, and ICMSE-CSIC Research Centers.

References

1. E.V. Clougherty, R.L. Pober and L. Kaufman, “Synthesis of oxidation resistant metal diboride composites”. Trans. Met. Soc. AIME 242 (1968), pp. 1077–82.

2. J.R. Fenter, “Refractory diborides as engineering materials”. SAMPE Quarterly 2 (1971), pp. 1–15.

3. Bull, J. D., Rasky, D. J. and Karika, C. C., “Stability characterization of diboride composites under high velocity atmospheric flight conditions”. 24th International SAMPE Technical Conference (1992), pp. 1092–106.

4. M.M. Opeka, I.G. Talmy, E.J. Wuchina, J.A. Zaykoski and S.J. Causey, “Mechanical, thermal, and oxidation properties of refractory hafnium and zirconium compounds”. J. Eur. Ceram. Soc. 19 (1999), pp. 2405–14.

5. S. R. Levine, E. J. Opila, M. C. Halbig, J. D. Kiser, M. Singh, J. A. Salem

"Evaluation of ultra-high temperature ceramics for aeropropulsion use", J. Eur. Ceram. Soc. 22 (2002), pp. 2757-67.

6. Chawla, K. K. and Chawla, N., "Processing of ceramic-matrix composites". ASM Handbook Vol. 21: Composites. ASM International, Metals Park, OH, 2001, pp. 589–99.

7. NIST Structural Ceramics Database, http://www.ceramics.nist.gov/srd/scd/scdquery.htm

List of Symbols, Abbreviations, and Acronyms

BSE – Backscattered Electrons

EDS – Energy Dispersive Spectroscopy

SE – Secondary Electrons

UHTC – Ultra High Temperature Ceramics

ZS – ZrB_2-SiC composite

ZSC - ZrB_2-SiC-C composite

ZSS - ZrB_2-SiC (fibers)-C composite

List of Tables

List of Figures

Figure 20 - Thickness of SiO_2 and ZrO_2 oxide layers as a function to exposure time for ZSC samples annealed in atmospheric air at 1400°C.

Figures and tables

Table 1

Acronym	ZrB_2 (%)	SiC (%)	C (%)
ZS	80	20	0
ZSC	56	14	30
ZSS	80 (matrix)	fibers	20 (matrix)

Table 2

	E (GPa)	υ	α (10^{-6} / °C)
ZrB_2	490	0.11	5.9 (300K) 8.4 (1500K)
α-SiC	480	0.16	5.3
C	910	-	1.0

Figure 1

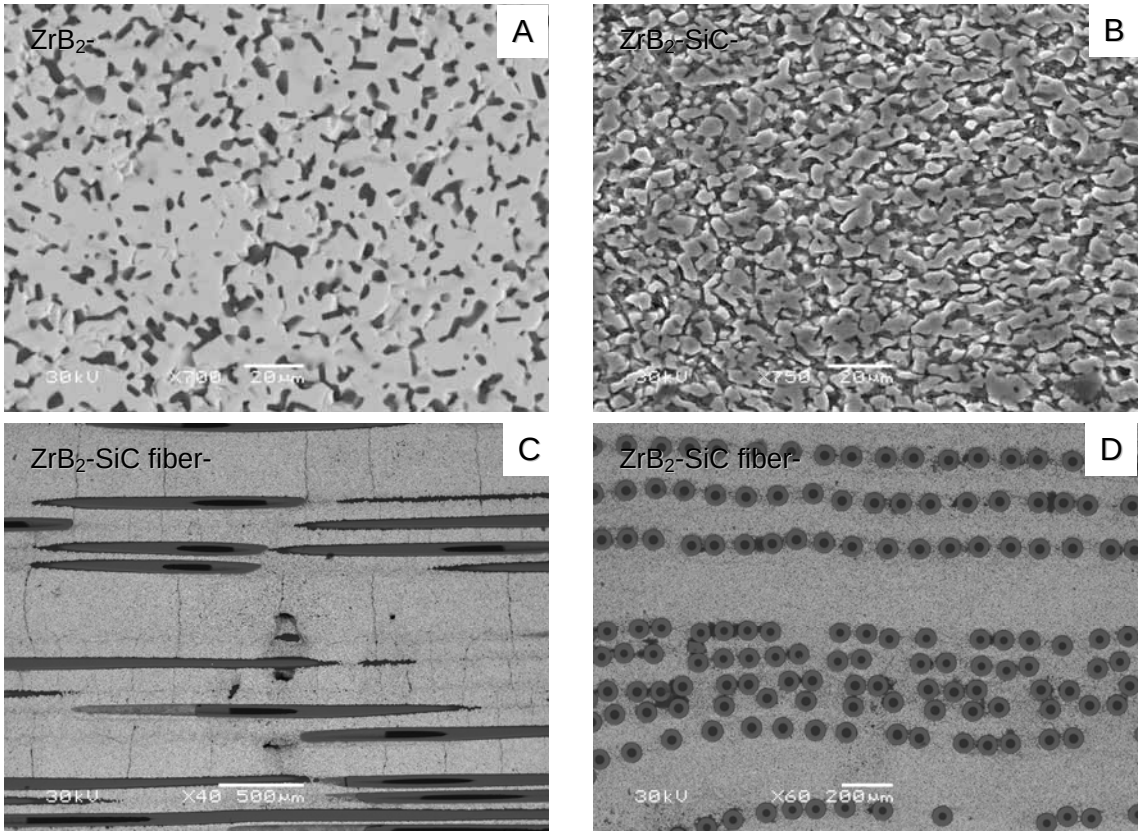

Figure 2

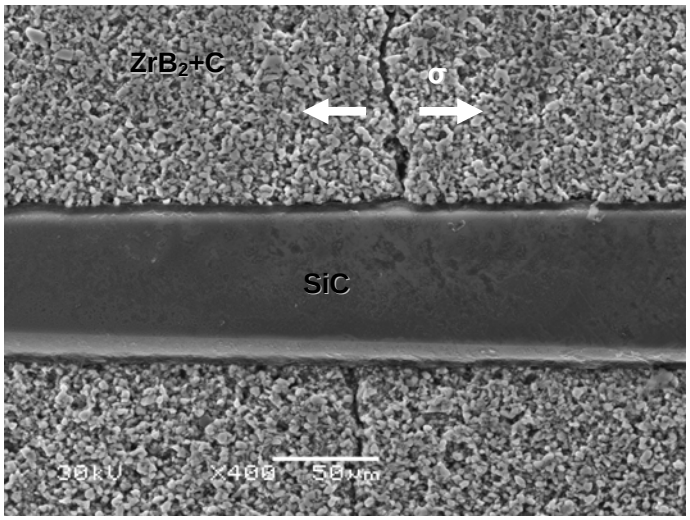

Figure 3

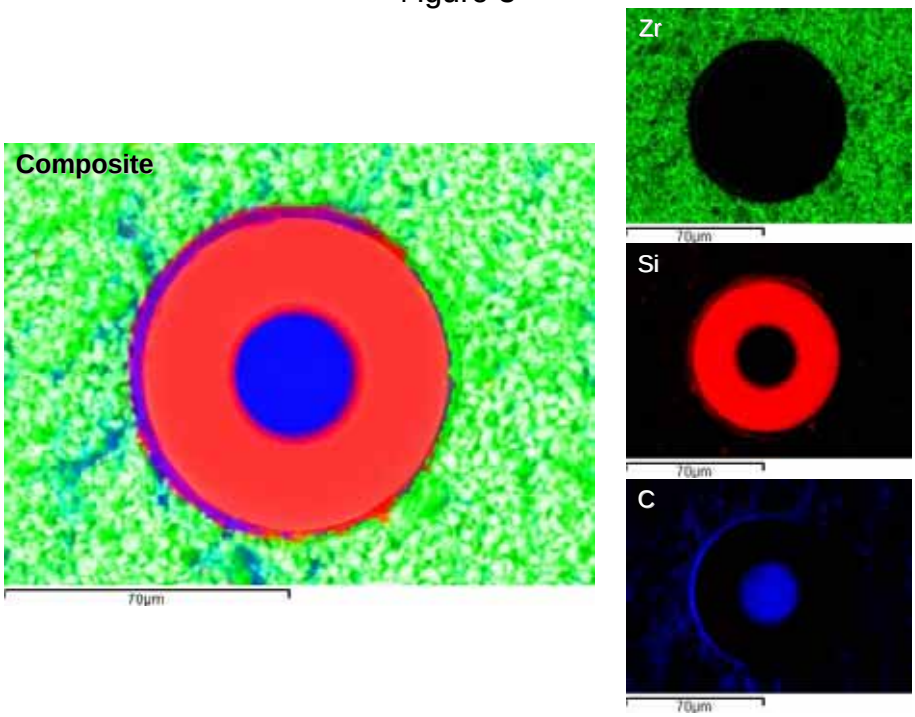

Figure 4

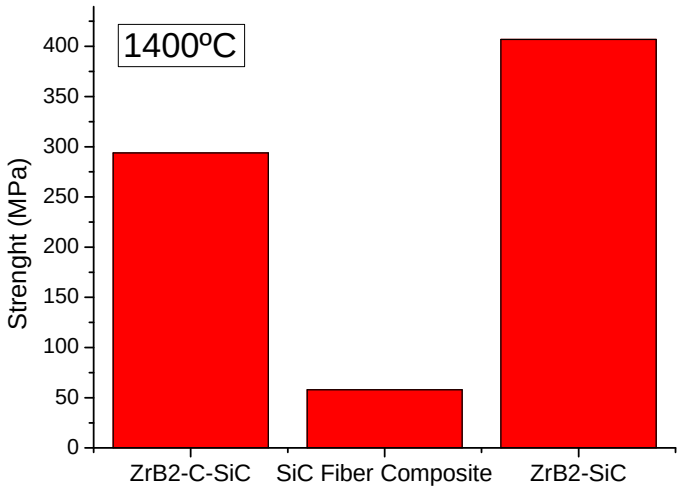

Figure 5

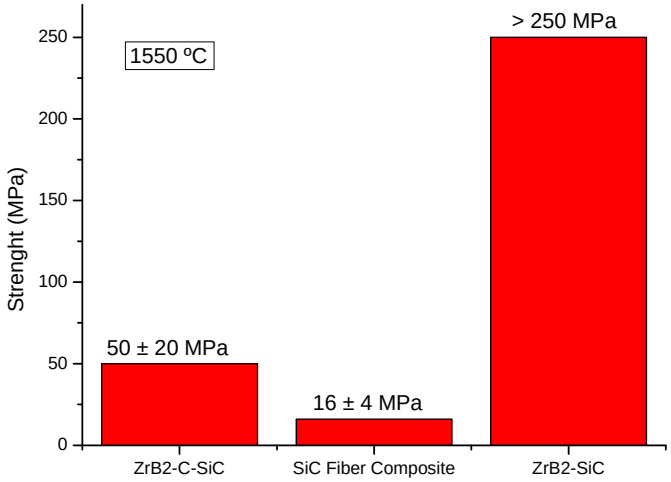

Figure 6

Failure Mode

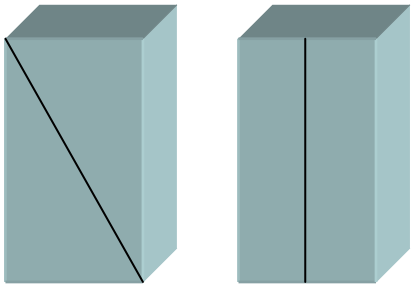

Figure 7

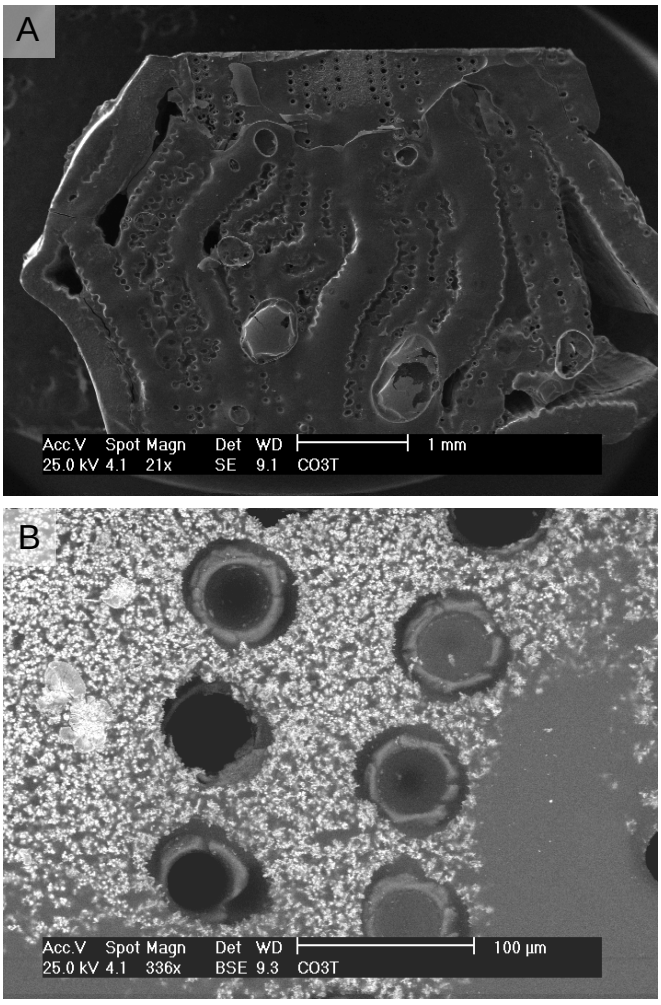

Figure 8

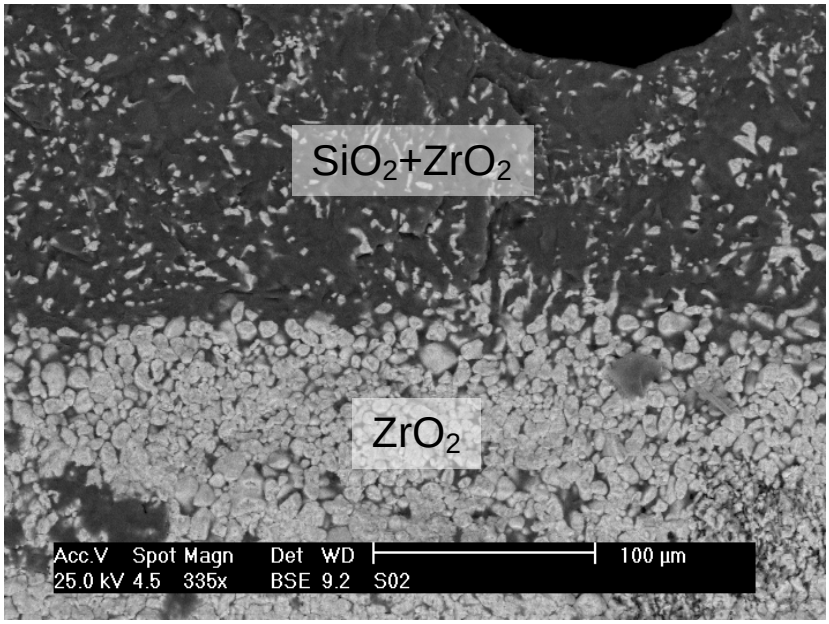

Figure 9

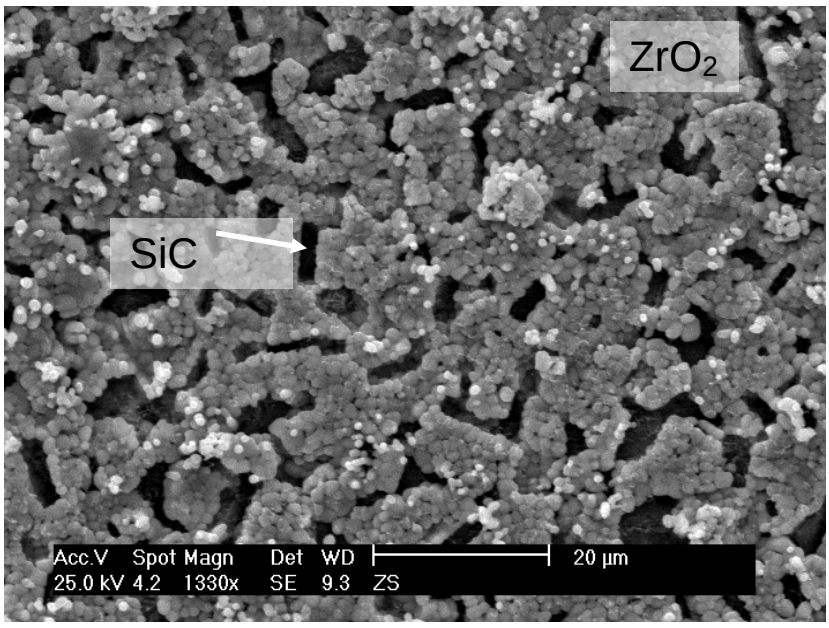

Figure 10

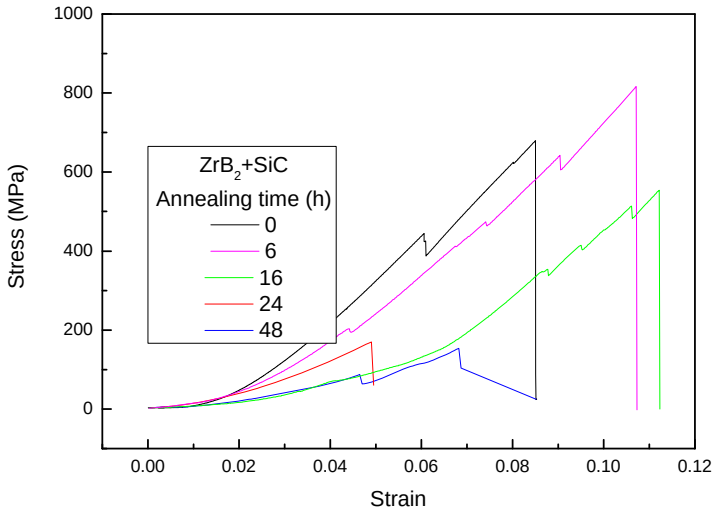

Figure 11

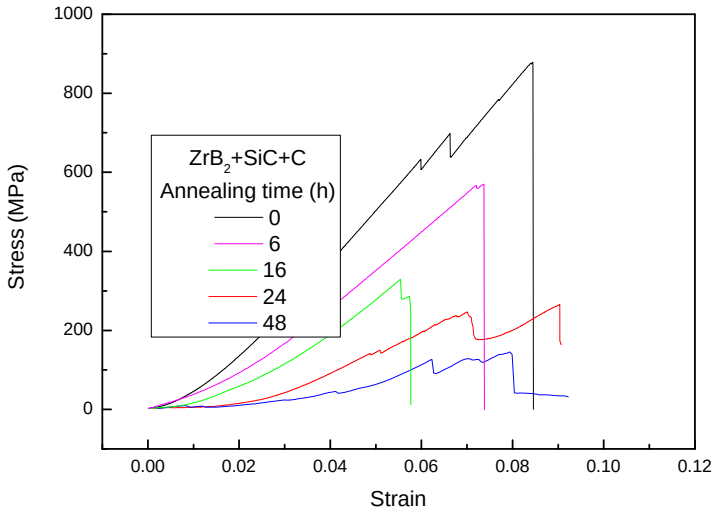

Figure 12

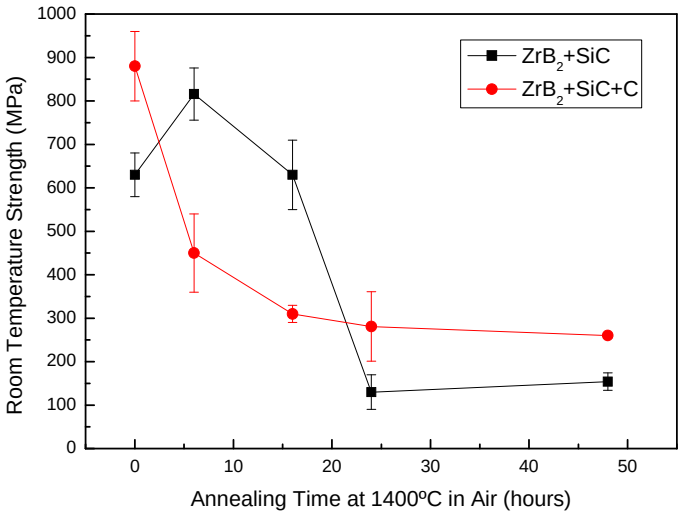

Figure 13

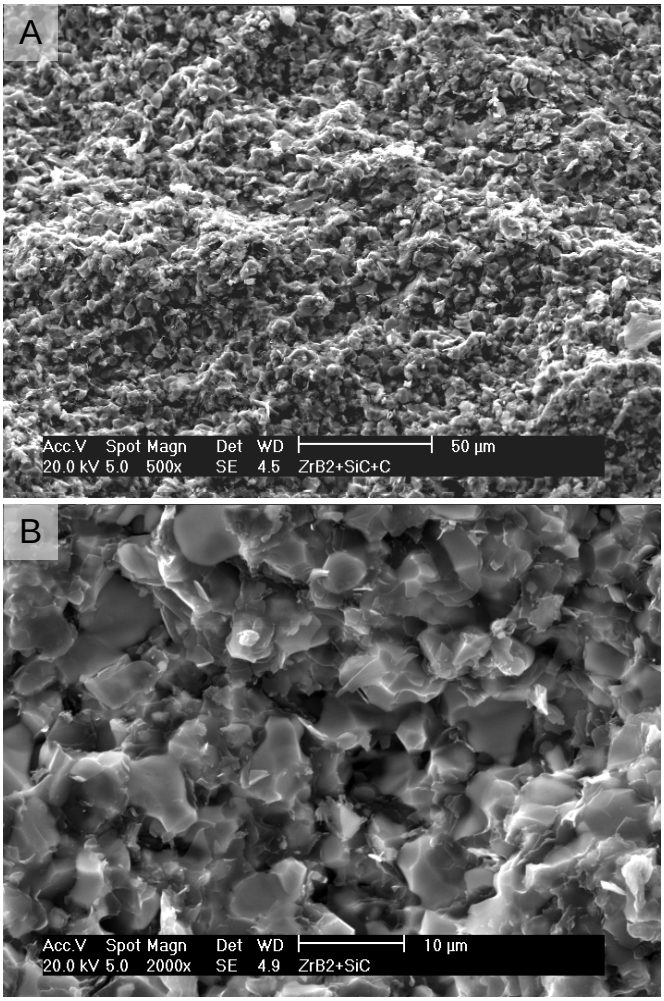

Figure 14

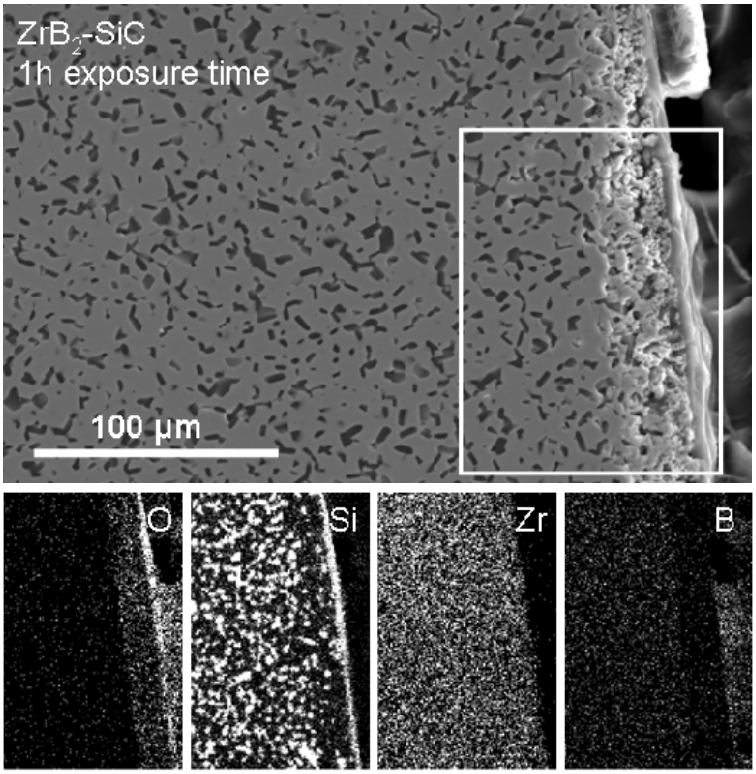

Figure 15

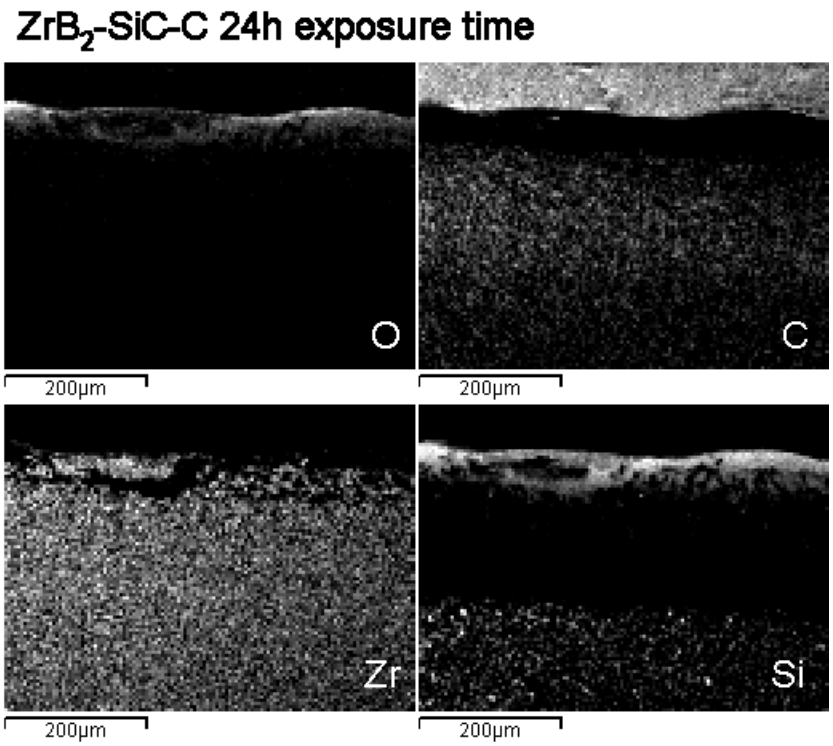

Figure 16

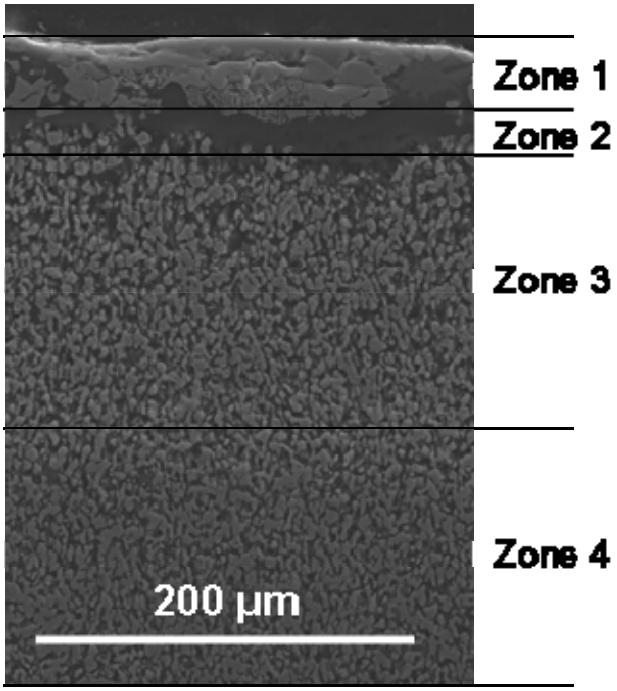

Figure 17

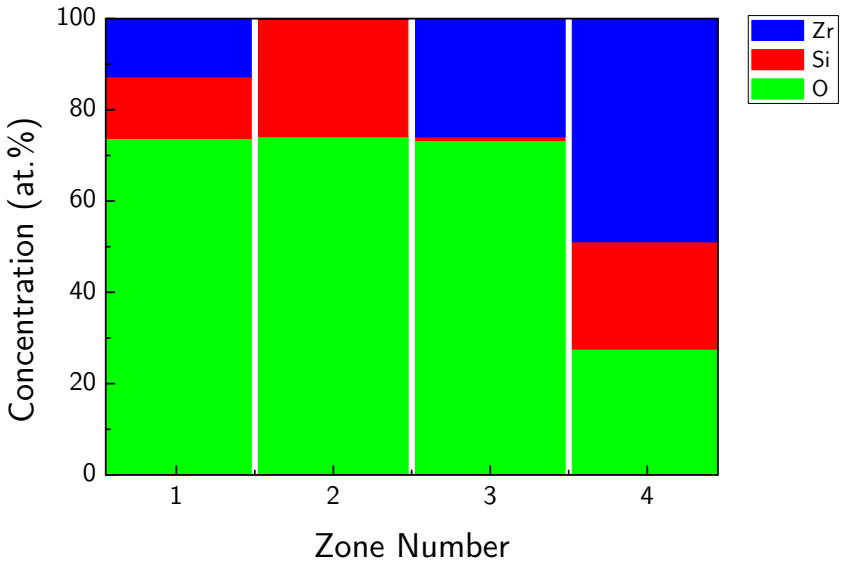

Figure 18

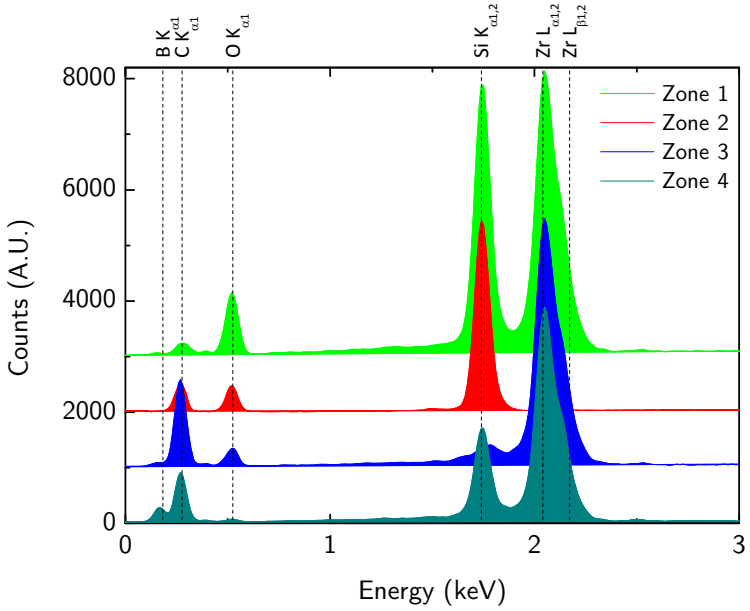

Figure 19

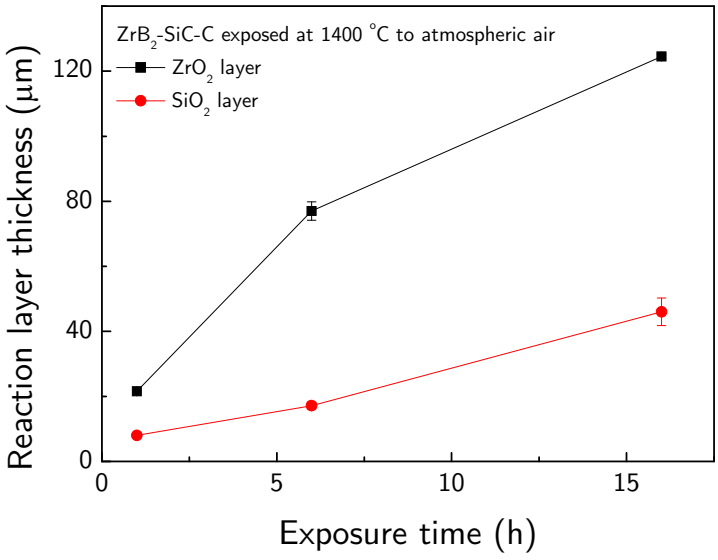

Figure 20

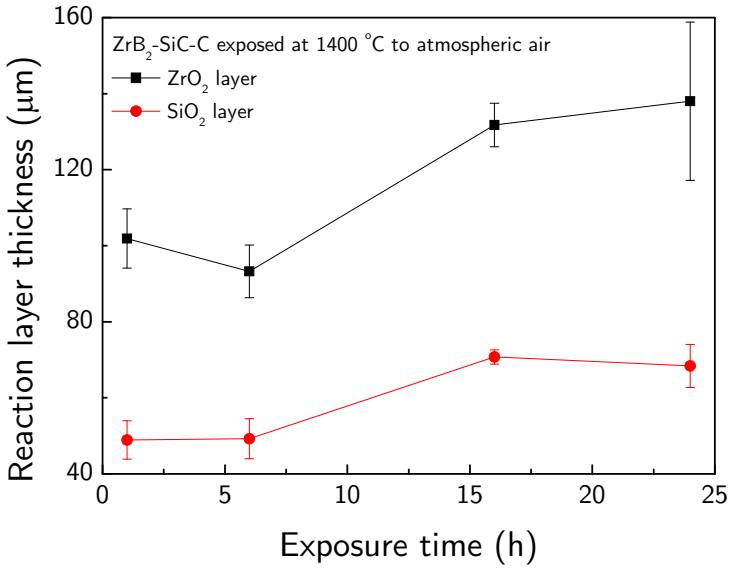
ZrB2-SiC-C exposed at 1400 °C to atmospheric air
ZrO2 layer
SiO2 layer
Reaction layer thickness (μm)
Exposure time (h)
160
120
80
40
0
5
10
15
20
25